Thomas, R., Davidson, P. (2010): Hambergite-rich melt inclusions in morganite crystals from the Muiane pegmatite, Mozambique and some remarks on the paragenesis of hambergite. - Mineralogy and Petrology, 100, 3-4, 227-239

DOI: 10.1007/s00710-010-0132-8

Hambergite-rich melt inclusions in morganite crystals from the Muiane pegmatite, Mozambique and some remarks on the paragenesis of hambergite

Rainer Thomas[1)] and Paul Davidson[2)]

[1)] **Deutsches GeoForschungsZentrum Potsdam, Telegrafenberg, D-14473 Potsdam, Germany**

[2)] **ARC Centre of Excellence in Ore Deposits, University of Tasmania, Hobart, Australia**

Correspondence:

Rainer Thomas, Deutsches GeoForschungsZentrum, Section 3.3 Chemistry and Physics of Earth Materials, Telegrafenberg, D-14473 Potsdam, Germany
E-mail: thomas@gfz-potsdam.de

Abstract

Raman spectroscopic studies of daughter crystals of hambergite [$Be_2BO_3(OH, F)$] in primary melt and secondary fluid inclusions in morganite crystals from the Muiane pegmatite, Mozambique, show that the inclusions have extremely high beryllium concentrations, corresponding to as much as 10.6 % (g/g) in melt inclusions and 1.25 % (g/g) BeO in fluid inclusions. These melt and fluid inclusions were trapped at about 610°C and 277°C, respectively. We propose two possible mechanisms for the formation of the hambergite crystals: (i) direct crystallization from a boron- and beryllium-rich pegmatite-forming melt or (ii) these are daughter crystals produced by the retrograde reaction of the boron-rich inclusion fluid with the beryl host, after release of boric acid from the primary trapped metastable volatile-rich silicate melt during cooling and recrystallization. Although we favour the second option, either case demonstrate the extent to which Be may be concentrated in a boron-rich fluid at relatively high temperatures, and in which species of Be may be transported. One important constraint on the stability of the hambergite paragenesis is temperature; temperatures of $\geq$650°C (at 2 kbar) hambergite is not stable and converts to bromellite [BeO].

Keywords: Morganite, fluid and melt inclusions, high Be concentration, hambergite, bromellite, miarolitic pegmatites

Introduction

High concentrations of otherwise rare elements are a common feature of some classes of pegmatites (Černý 1982). Prokofyev et al. (2003) demonstrated that strong enrichment of boron as boric acid [H_3BO_3] is a characteristic of some pegmatite types worldwide. Moreover, Thomas et al. (2008b) demonstrated high concentration of Rb and Cs together with high boron concentrations as boric acid and alkali pentaborates in a graphic pegmatite from the Island of Elba, Italy. Likewise, pegmatites can have high concentrations, up to ore-grade, of Be, Nb, Ta, Zr, and several other metals (Černý 1982). However, the mechanism or mechanisms by which such high concentrations can be achieved remain under debate.

This study examines beryl from the Nb-Ta-REE-U granite pegmatites in the Alto Ligonha region of Mozambique, currently mined for tantalum and gemstones (topaz, herderite, tourmaline and beryl). During this study primary crystallized melt inclusions were observed to contain large hambergite daughter crystals. Information on the geology, mineralogy, geochemistry and inclusion work of the Alto Ligonha region are given in Fung et al. (1990), Felix and Kiessling (1990), Lächelt (1990), and Schmidt and Thomas (1990a, b), Gomes et al. (2009). These large daughter crystals have high Be and B contents, since hambergite contains 53 % (g/g) BeO, and 36 % (g/g) B_2O_3, with variable water and fluorine. Such high Be concentrations could be the result of a post-trapping process, and for reasons to be discussed we favor this explanation. In this study we test our own hypothesis that these inclusions may demonstrate one mechanism for dissolving high concentrations of Be in common pegmatite-forming environments, especially those enriched in boron. Moreover, there is no reason to assume this mechanism to be restricted to post-entrapment processes. The results obtained

from inclusions shed light on the importance of down-temperature changes in stability and solubility of phases that can occur on a macroscopic scale in pegmatite system.

Samples

For this study we used a doubly polished section (30 x 25 x 2 mm) of a morganite crystal (pink colored beryl) from the Muiane Ta-Nb-Li-pegmatite in Alto Ligonha region, Mozambique. The sample comes from the core zone of a pegmatite, and was found together with graphic potassium feldspar, microcline, albite, quartz, green and red tourmaline, beryl, petalite and muscovite (Schmidt 1986).

The almost water-clear morganite crystal from the Muiane pegmatite contains a small number of large, randomly distributed volatile-rich melt inclusions (with diameters up to 875 μm). Careful examination reveals that the inclusions are arranged in growth zones marked by tiny submicrometer sized inclusions. Around all large inclusions there is halo free from fluid inclusions. There are no indications that the large hambergite-bearing inclusions were formed by necking down or similar processes.

Homogenization measurements on the large primary inclusions (Schmidt and Thomas 1990a) using a parallel section of the same sample gave a melting temperature of 610 ± 27°C (number of studied inclusion n = 30). Other secondary fluid inclusions homogenize at 277 ± 5°C (n = 10) into the liquid phase.

For comparison and as a Raman reference standard we used a colorless hambergite crystal (2 x 2 x 1.5 cm) from the Rangkul pegmatite field, eastern Pamirs, Tadzhikistan with about 6.4 % (g/g) F, 35.3 % (g/g) B_2O_3 and 54.8 % (g/g) BeO. A description of this miarolitic pegmatite is given by Peretyazhko and Zagorsky 1999; Zagorsky and Shmakin 1999. Paragenetic minerals of the colorless to white, up to 10 cm hambergite crystals, sometimes with lilac terminations, are microcline, lepidolite, pale pink beryl, polychrome tourmaline,

rubellite, topaz, danburite, and fluorite. The hambergite crystal used for comparison is characterized by many fluid inclusions and melt inclusions – all very rich in boric acid. The fluid inclusions contain daughter crystals of ramanite-(Cs) and nahcolite in addition to boric acid (Thomas et al. 2010).

A further hambergite crystals (1.5 x 0.4 x 0.3 cm) used as Raman reference comes from a miarolitic pegmatite in the Malkhan pegmatite field in the Transbaikal region with 1.4 % (g/g) F, 38.3 % (g/g) B_2O_3, and 50.2 % (g/g) BeO (Peretyazhko and Zagorsky 1999, Zagorsky and Shmakin 1999). Paragenetic minerals here are microcline, smoky quartz, lepidolite, rubellite, beryl, and danburite.

Additionally, as a well characterized reference for Raman measurements we used a piece of a large hambergite crystal (24.3 g) from the Anjanabonoina pegmatite, Madagascar (# 102984 from the Harvard Mineralogical Museum; Dyar et al. 2001). This sample contains 0.78 ± 0.04 % (g/g) F (Rhede, oral communication), 37.57 ± 0.86 % (g/g) B_2O_3, and 51.45 ± 1.22 % (g/g) BeO.

Inclusion petrography

Inclusions in morganite from Muiane

The mean diameter of 25 melt inclusions in the morganite sample from Muiane is 270 $\pm$ 85 µm, smaller melt inclusions are rare. The largest inclusions in the sample have dimensions of 405 x 240 x 350 µm and 1150 x 700 x 440 µm, respectively. All melt inclusions contain large hambergite daughter crystals [Be_2BO_3(OH, F)] (Fig. 1a); and smaller daughter crystals of quartz, cristobalite, beryl (up to 5 % (vol/vol)), B-muscovite, topaz, sassolite, apatite, calcite and phenakite; a saturated solution high in boric acid, and a large bubble. In all cases in this study daughter mineral identification was by Laser Raman spectroscopy. This assemblage shows the melt to have been rich in silica, water, Be, F, and carbonate.

Secondary fluid inclusions (up to 100 x 20 x 15 μm) (Fig. 1b) on healed fissures cross-cutting the growth zones with homogenization temperatures of (277 ± 5°C) contain a saturated boric acid solution with small hambergite daughter crystals, cristobalite, polylithionite and small needles of arsenolamprite [native As].

Inclusions in hambergite from Rangkul

At room temperature the sample contains fluid and primary melt inclusions. The fluid inclusions contained daughter crystals of ramanite-(Cs) and nahcolite in addition to sassolite [H_3BO_3] (Fig. 2a). The primary melt inclusions are characterized by a vapor bubble, generally deformed, a small amount of a water-rich solution, and a large volume (~60 % (vol/vol)) of sassolite (see Fig. 2b and Appendix Fig. 7).

Analytical methods

Raman spectroscopy

In this study we used Raman spectroscopy as the principal tool for the identification of the daughter mineral phases inside the inclusions as well as for the estimation of the boron concentration. Raman spectra were obtained with a Jobin Yvon LABRAM HR800 confocal-Raman spectrometer (grating: 1800 and 2400 gr/mm) equipped with a Peltier-cooled (-70°C) CCD detector and an Olympus optical microscope with a long-working-distance LMPlanFI 100x/0.80 objective. We used the 514 and 488 nm excitation of a Coherent Ar^+ laser Model Innova 70C, a power of 300 mW (about 14 mW on sample). For the low-frequency range we used edge filters. Each unpolarized spectrum represents the accumulation of six acquisitions of 20 s each. The spectra were collected at a constant laboratory temperature (20°C). The positions of the Raman bands were controlled and eventually corrected using the principal plasma lines in the Argon laser (Craig and Levin 1979). The recommended and measured

positions of the plasma lines in the fingerprint spectral region are not larger than 0.6 cm^{-1} using a pinhole aperture of 100 μm.

Raman identification criteria

The main daughter mineral in inclusions in the Muiane morganite is hambergite [$Be_2BO_3(OH, F)$] and its identification with Raman is simple and unambiguous (Downs 2006) – see Appendix Fig. 8, and is confirmed by comparison to the previously described hambergite reference samples.

The concentration of boron in the inclusions and water in the inclusion glass was estimated by Raman analysis according to Thomas (2002), Schmidt et al. (2005), Thomas and Davidson (2006) and Thomas et al. (2006).

Due to overlap between the major and minor spectral bands of the host minerals in this study (morganite and hambergite), and contained daughter phases in inclusions, some of the characteristic bands of the daughter phases are hidden by the host spectra. For this reason we use the following spectral bands as characteristic of the named minerals: Sassolite, very strong Raman bands at 500, 880, 3165, and 3247 cm^{-1}, and weak bands at 186.5 and 211 cm^{-1}.

Li tetraborate (diomignite), a strong band at 1028 cm^{-1} and weaker features at 390, 446, 544, 1097 and 1352 cm^{-1}. Na tetraborate, strong bands at 575 and 1036 cm^{-1}, and weaker bands at 385 and 461cm^{-1}. Ezcurrite [$Na_4B_{10}O_{17} \cdot 7H_2O$], strong bands at 476, 512.5, 570.4, 760**,** 878.9 and 1040.4 cm^{-1}, and weak bands at 663, 678.8 cm^{-1}. Bromellite shows a triplet at 678, 684, and 722 cm^{-1} and further bands at 388, 1081, and 1097 cm^{-1}.

Cold-seal pressure vessel homogenization experiments

Because the melt inclusions in morganite were completely crystallized and contain different mineral phases, a saturated fluid and a CO_2-rich vapor bubble, it was necessary to re-homogenize the inclusion to a homogeneous, daughter crystal-free glass to demonstrate that

the primary inclusions were trapped as volatile-rich melt droplets at high temperatures. For this we used the conventional horizontal cold-seal pressure vessel technique (Thomas 2000, Thomas et al. 2008b).

Doubly polished plates of morganite were placed into an open Au capsule (30 mm long, 5 mm diameter) together with a small emerald crystal from the Lened Emerald Prospect, Northwest Territories, Canada with B-free, CO_2-rich fluid inclusions only (Marshall et al. 2004). The emerald was added to each charge to test the effect of heating on B-free fluid inclusions, since we hypothesized that beryl is highly soluble only in hot B-rich fluids. The vessel was pressurized with CO_2 to 2 kbar, and the sample moved into a 650°C preheated furnace. The run time was 20 hours. After the experiment the Au capsule was removed from the furnace and quenched isobarically with compressed air. After quenching, the samples were removed, cleaned and re-polished for the Raman microprobe study. One piece of morganite, re-homogenized at 650°C was further heated to 675°C and 2 kbar.

Because of the high concentration of Be, B, C, H_2O, and Li in the inclusion glass it is highly unstable under an electron beam, so microprobe analyses of the glass could not be performed.

Microthermometry of melt inclusions

Some microthermometric reconnaissance measurements on melt inclusions in hambergite from the Rangkul pegmatite field were performed using a calibrated LINKAM THMS 600 heating and freezing stage, together with a TMS92 temperature programmer and a LNP2 cooling system mounted on an Olympus microscope. The stage was calibrated with synthetic fluid inclusions (SYNFLINC) and melting points of different standards. All measurements were performed under argon. The standard deviation depends on absolute temperature and is always less than $\pm$ 2.5°C for temperatures greater 100°C, and is $\leq$ 0.2°C for cryometric measurements lower than 20°C. Samples were 300-µm-thick, doubly polished hambergite

chips. To prevent decrepitation during excessively rapid heating, the homogenization runs were performed with a constant heating rate of 5°C/minute.

Results

Estimation of compositions of inclusion in morganite

By a conservative visual estimate the primary melt inclusions contain about 6.6 ± 1.8 % (vol/vol) hambergite (mean and 1σ from 23 inclusions), corresponding to 8.3 ± 2.3 % (g/g) BeO or 3.0 ± 0.8 % (g/g) Be and about 10.1 ± 2.8 % (g/g) H_3BO_3 determined with Raman spectroscopy. Beryl forms small separate daughter crystals in the Muiane inclusions, which have highly variable phase ratios up to 5% (vol/vol). However this volume varies widely from inclusion to inclusion, therefore the volume of the "daughter beryl" was not taken into account in this calculation; therefore total Be-concentrations are somewhat higher than stated.

By contrast, the estimated hambergite volume in the associated fluid inclusions (~ 1% vol/vol) corresponds to about 1.25 % (g/g) BeO or 4500 ppm Be in the inclusions (Fig. 1b) and an additional of 1.5 % (g/g) H_3BO_3 to the 5.5 % in the solution, giving a total of 7 % (g/g) H_3BO_3.

To put these concentrations into perspective this data means that some of the Muiane hambergite-bearing inclusions contain up to 38,000 ppm Be. This demonstrates that Be and B concentrations in melt inclusions in morganite are enriched by a factor of about 10^3 to 10^4 over their average abundance in typical granites. These results are consistent with measurements from another locality (Thomas et al. 2010).

Raman spectroscopy of hambergite

There is remarkable agreement of the strongest band in the Raman spectra between the hambergite daughter crystals in morganite from Muiane (153.2 cm^{-1}), and the hambergite

crystals from Anjanabonoina, Madagascar (155.4 cm^{-1} according to RRUFF No. R050672) with about 0.8 % (g/g) F, and from Malkhan (156.4 cm^{-1}) with 1.4 % (g/g) F (Peretyazhko and Zagorsky 1999). By contrast the hambergite crystals from the Rangkul pegmatite field, eastern Pamirs, Tadzhikistan with about 6.2 % (g/g) F have their strongest Raman band at 150.0 cm^{-1}. This implies that the Muiane hambergite daughter crystals have a composition of Be_2BO_3(OH, F) and argues for the participation of fluorine in moderate concentrations (3.3 % (g/g) F) during their formation (see Appendix Fig. 9).

Cold-seal pressure vessel homogenization experiments

Melt inclusions in hambergite from the Rangkul pegmatite

Reconnaissance homogenization measurements on 10 primary melt inclusions in hambergite from the Rangkul pegmatite yielded a homogenization temperature of 581 ± 15°C (see Appendix Fig. 7). At room temperature the inclusions contain a large sassolite crystal, a small amount of a water-rich solution and a vapor bubble. Homogenization is to the liquid phase. The melting temperature of sassolite is 159 ±15°C (n = 17), which according to Gmelin (1954) corresponds to ~72 % (g/g) H_3BO_3 or ~40 % (g/g) B_2O_3 as a first approximation, because the influence of fluorine on the melting behavior on boric acid is unknown. Such high boron concentrations (here as a low-viscous melt) may be the first description for a pegmatite system.

The viscosity of the melt at the homogenization temperature is presumably similar to water because the last small vapor bubble in the inclusions rapidly oscillates back and forth. Some large inclusions (diameter >50 μm) partially decrepitated, and their molten contents flowed out onto the surface. Raman measurements on such melt droplets, which at room temperature are a metastable glass, give relatively high concentration of fluorine as $[BeF_2]^{2-}$ which could be detected in the boric acid glass by the presence of the strong ν_1 band at 547 cm^{-1}; (the weak bands at 255 (ν_2), 385 (ν_4) and 800 (ν_3) cm^{-1} are partially concealed, Piriou et al. 1981). This

means that the boron-rich melt batches in the miarolitic pegmatites from the Rangkul field contain significant amounts of fluorine which forms the BeF_2^{2-} complex, a very reactive compound at high temperatures.

Also according to experiments (e.g. Tang et al. 2001; McMillen and Kolis 2008), BeO in fluorine- and boron-rich systems is readily soluble in flux-rich melts or concentrated hydrothermal solutions and forms K_2BeF_4 as a main component, which is also the starting material for the hydrothermal growth of high-quality crystals of $KBe_2BO_3F_2$ as solid-state laser sources for the deep UV region (e.g., Tang et al. 2001; Ye and Tang 2006). At high temperatures (~600°C) and high concentrations together with boric acid and water, hambergite is formed by the following reaction:

$$2\ K_2BeF_4 + H_3BO_3 + H_2O = Be_2BO_3(OH) + 4\ HF + 4\ KF \qquad (1)$$

Melt and fluid inclusions in morganite from the Muiane pegmatite

The feasibility of our interpretation regarding the origin of the hambergite daughter crystals can be demonstrated by the cold-seal pressure vessel homogenization experiment. In this experiment all hambergite crystals in the inclusions dissolved and were replaced by 3 % (vol/vol) bromellite [BeO] crystals, corresponding to about 7.3 % (vol/vol) hambergite (Fig. 3). This is a further proof that our interpretation of the Raman spectra was correct. The hambergite is transformed into bromellite [BeO], a very rare mineral (Grew 2002 and Černý 2002), according to the following reaction:

$$Be_2(OH)[BO_3] + H_2O = 2\ BeO + H_3BO_3 \qquad (2)$$

Thus hambergite is not stable at 650°C and 2 kbar (the temperature and pressure of the homogenization experiment). This is an important constraint on the process of hambergite formation, since it implies an upper temperature limit to hambergite stability, not previously recorded in the literature. Furthermore the rapid formation of bromellite at temperatures

greater than 650°C by the decomposition of hambergite, or by the reaction of the fluid with the beryl host, demonstrate that under such conditions Be is extremely mobile.

Concurrently with dissolution of the hambergite crystals during cold-seal homogenization experiments in large inclusions the boron concentration increases significantly, indicated by daughter crystal of sassolite, which can be clearly identified by Raman spectroscopy. The melting temperature of the sassolite crystals in the volatile-rich melt inclusions is 59.7 ± 0.6°C (n = 6). This temperature corresponds to a boric acid concentration of 12.9 ± 0.2 % (g/g) H_3BO_3 in pure water. From the intensity ratio I = (876/3400 cm^{-1}) = 0.114, determined with Raman spectrometry, the boric acid concentration in the liquid phase is 10.3 % (g/g) (Thomas, 2002). Since only 4.8 % (g/g) H_3BO_3 can be dissolved in water at 20°C, the excess boron (10.3 – 4.8 % = 5.5 %) must be combined with alkali borates (Gmelin 1954). According to Raman spectroscopy the main phases in the inclusion liquid are Li tetraborate (diomignite) [$Li_2B_4O_7 \cdot 5\ H_2O$], Na tetraborate, and ezcurrite [$Na_4B_{10}O_{17} \cdot 7H_2O$]. During our Raman work on the Muiane sample we found a highly soluble mineral phase with a Raman spectra characteristic of diomignite, the existence of which as a true mineral species has been disputed. The high solubility during the spectroscopic measurements, and the high boric acid concentration in the inclusion, can be regarded as a second confirmation of the mineral diomignite. For discussion see London et al. 1987, and the Appendix. An estimation of bulk H_3BO_3 concentration is about 18.4 % (g/g), this would correspond to a maximum of about 11.8 % (vol/vol) hambergite.

Small melt inclusions completely homogenize to a water-rich silicate glass (Fig. 4), which, however, dissociated during quenching into a water-rich glass (6.6 $\pm$ 0.2 % (g/g) H_2O – determined with Raman spectroscopy using 8 melt inclusions) and a fluid sub-phase containing a water-rich liquid and a CO_2-rich bubble. The bulk water concentration of the whole inclusion is about 45 % (g/g) and the bulk density 0.94 g/cm^3. In such melt inclusions

practically all the boron is now in the glass and the Be is left in the liquid phase as bromellite which forms stable crystals, identified by Raman spectroscopy.

During further heating to 675°C at 2 kbar the internal pressure in the inclusions increased slightly relative to the confining pressure, which produced halos of new fluid and melt inclusions around large volatile-rich melt inclusions, demonstrating the high mobility of the melt and fluid phase at this temperature. These halos are concentric around large single inclusions with bromellite-bearing inclusions near the central inclusion, but only fluid inclusions in the outer fringes (Fig. 5a). Intact bromellite-bearing inclusions contain the following phases: bromellite, silicate glass, water-rich liquid, and CO_2-rich vapor (Fig. 5b). However, most bromellite-bearing inclusions have decrepitated and lost the mobile phases (liquid and vapour) into the outer region (Figs 5c-d). The inclusion arrangement in the halos resembles a circular chromatogram. The pressure difference was not so high that total decrepitation of surface-near inclusions occurs. Each newly formed melt inclusion near the centre contains bromellite crystals (Figs. 5b-e), but never other mineral phases, suggesting that bromellite was mobilized via the H_2O-vapor from the central inclusion according to the following simplified reaction:

$$BeO\ (s) + H_2O(g) = Be(OH)_2(g), \qquad (3)$$

showing that the hydroxide $Be(OH)_2$ is transported very easily by vapor (see also Newkirk and Smith, 1965). The last reaction will reverse during cooling. Note however, that the volume of the bromellite crystals increases strongly with temperature. The volume of bromellite is larger than the corresponding beryl volume of the inclusion. This means that not only the initial hambergite crystals, but also the host, were the source of the new-formed bromellite. Beryllium hydroxide can transport large amounts of CO_2, which is then released during crystallization of bromellite. Figures 5b, c and e suggest, indirectly, that bromellite

was transported via beryllium hydroxide (equation 3), because of the extreme solubility of CO_2 in beryllium hydroxide (Gmelin 1930, p. 94). During cooling and crystallization the CO_2 is released again.

That bromellite was not only formed by the decomposition reaction of hambergite can be seen from large fluid inclusions which originally contained 1% (vol/vol) hambergite. After heating to 650°C the bromellite volume increased to about 10% (vol/vol) (Fig. 6). This also demonstrates that the boric acid concentration is not stoichiometricaly related to the amount of bromellite: at high temperatures boric acid react as catalyst for the decomposition of beryl.

That boron is responsible for the decomposition reaction of beryl can be seen at the fluid inclusion in the Lened emerald added to the cold-seal pressure vessel homogenization experiments charge. After the run at the same conditions the fluid inclusions do not contain crystals of bromellite.

Discussion

The foregoing results demonstrate that melts or fluids trapped in the Muiane inclusions represent an extremely Be, B, and H_2O-rich material, with moderate F concentrations, and that there were complex interactions of the different species in solution with the host during cooling. However, this leaves open the question of whether these inclusions are primary or the product of secondary reactions during cooling. Daughter crystals of hambergite were found in morganite only, coeval crystals of quartz and tourmaline (rubellite) at the same point in the paragenetic sequence contain only high boric acid concentrations, indicated by large sassolite daughter crystals, but never hambergite. A possible interpretation is that hambergite was formed by the reaction of the boric acid- and fluorine-rich fluids in the morganite host after trapping and during cooling. The absence of hambergite in simultaneously crystallizing quartz and tourmaline argues against the alternative model; i.e. trapping of an initially strongly Be-rich melt/fluid. However, the formation of free-grown hambergite crystal in other

miarolitic pegmatites (Pamir, Malkhan) with very high H_3BO_3 concentration in the inclusions (Appendix Fig. 7**)** demonstrates that in some cases the Be concentration can reach concentrations allowing direct crystallization of hambergite from the melt.

Relatively high fluorine concentration in the system is indicated by daughter crystals of topaz in melt inclusions in morganite, and occasionally by potassium tetrafluoroborate [KBF_4] with the strong ν_1 band at 774 cm^{-1} (Bates and Quist 1975) in primary inclusions in beryl and quartz crystals, as well as chiolite [$Na_5Al_3F_{14}$] and cryolithionite [$Na_3Li_3Al_2F_{12}$] as daughter minerals in some fluid inclusions in quartz. The following simplified reactions show two possible paths from beryl to hambergite consistent with the principal daughter minerals (mica, topaz) found during this study:

$$2\ Be_3Al_2Si_6O_{18} + 3\ H_3BO_3 + 2\ K_2CO_3 = 3\ Be_2BO_3(OH) + 4\ KAlSi_3O_8 + 2\ CO_2 + 3\ H_2O \quad (4)$$

the microcline ($KAlSi_3O_8$) then reacts in the water-rich system to form muscovite, and

$$2\ Be_3Al_2Si_6O_{18} + 3\ H_3BO_3 + 4\ HF = 3\ Be_2BO_3(OH) + 2\ Al_2SiO_4(F_2) + 10\ SiO_2 + 5\ H_2O \quad (5)$$

For reasons already stated, we consider the hambergite as a secondary daughter mineral phase in the inclusions formed after trapping by reaction of the boron- and fluorine-rich reactive fluid with the host, rather than primary (crystallized directly from a mineral-forming fluid or melt). However, the mechanism is the same in either case, its existence demonstrating clearly that Be, together with carbonates and/or fluorides, can be enriched in boron-rich systems to unusually high concentrations at temperatures of pegmatite crystallization (see Thomas et al. 2010).

The boron-rich and fluorine-bearing fluids trapped in the Muiane pegmatite inclusions have a high solution capacity for Be, underlined by the extremely large dimensions of the

hambergite daughter crystals. Note that the inclusion size depends on the solubility of the host as well as from the rate of crystallization (Baker 2008). Such B-rich and F-bearing fluids are common in pegmatite-forming environments (e.g., Thomas et al. 2003, 2009; Thomas and Davidson 2008), as indicated by the B- and F-rich minerals (tourmaline, topaz, zinnwaldite, muscovite and others) common in some pegmatites, and the presence of B- and F-rich melt and fluid inclusions found in many pegmatites (Thomas and Davidson 2008). In this context we note that a significant proportion of pegmatite beryl crystals in the gem trade are described as "hydrothermally etched" or just "etched". These show clear corrosion and partial dissolution consistent with attack by a reactive fluid. We would argue that a similar reaction has occurred between B-rich fluid inclusions and their host morganite in the Muiane pegmatite, but here all of the phases involved are trapped and preserved.

We would also like to note the occurrence of hambergite crystals described in Switzer et al. (1965) from the Himalaya mine, Mesa Grande, San Diego County, California, where they were reported to have been found as a large numbers of very small unattached crystals in a pegmatite cavity with corroded beryl crystals, and only in those cavities which contained beryl.

This being the case there may be a transitory, although still magmatic mechanism via reactive boron-rich solutions by which, at relative high temperatures, such fluids can partly or completely dissolve small dispersed beryl crystals, increasing the Be concentration further, and may form the basis for the crystallization of larger beryl or Be-bearing crystals during subsequent cooling, possibly at some distance from the site of dissolution. At, or near, maximum Be-solubility this may be compared to Ostwald ripening, large crystals, with their greater volume to surface area ratio, represent a lower energy state. Thus, many small crystals will attain a lower energy state if transformed into large crystals.

Given the absence of hambergite in syn-paragenetic quartz and feldspar it seems probable in this case that the high Be content in the inclusions comes from the reaction of the boron-

rich and fluorine-bearing fluid with their morganite host after trapping. This suggests that the dissolution results from a change in speciation during cooling, and thus the reactivity of pegmatite fluids can fluctuate widely during their evolution down-temperature, as do solubilities. This temperature dependence of Be-solubility is demonstrated by the primary and secondary inclusion, which shows that the solubility of Be is high and decreases with decreasing temperature dramatically. In our case from a mean of 30,000 ppm Be at 610°C (primary inclusions) down to 4,500 ppm at 277°C (secondary fluid inclusions).

Concluding Remarks

In this study we have demonstrated that Be can have exceptionally high solubility in naturally occurring B-rich pegmatite fluids. Moreover, this study suggests that fluctuations in Be solubility and mineral stability in such fluids can be extremely wide over rather small temperature ranges (up to a factor of 10 between 600 – 300°C), and can have important repercussions in mineral formation and dissolution as they cool.

This study suggests that the hambergite crystals observed in melt and fluid inclusions either crystallized directly as a daughter mineral at high temperatures ($\leq$ 600°C) or grew during the retrograde cooling and dissociation of the primary melt, in this case in melt inclusions, into different mineral phases and boric acid-rich fluid, which reacted with the host mineral. In both cases the inclusions were trapped at high temperatures. The study shows also that a boric acid-rich fluids and/or melts can, at relatively high temperatures, transport Be in high concentrations. If fluorine is present, Be forms stable [BeF_2^{2-}] complexes, which substitute into the hambergite lattice for OH. This study demonstrates that free-grown hambergite in miarolitic pegmatites commonly is a high temperature mineral. However, due the high solubility of beryl in boric acid-rich fluids hambergite can also crystallize at moderate temperatures (200 – 300°C) as demonstrated in the Muiane pegmatite fluid inclusions.

Furthermore, at higher temperatures (>600°C) hambergite is not stable and dissociates into bromellite. Bromellite is reactive, and during cooling, may undergo retrograde reaction with other elements, e.g, in boron-rich fluids to produce hambergite (reaction 4) or other Be minerals, which may explain the rarity of bromellite in nature.

The formation of the volatile beryllium hydroxide at high temperatures as an intermediate phase shows a further possibility for the transport form of beryllium in the pegmatite stage.

Appendixes

Hambergite from the Rangkul pegmatite field, eastern Pamirs, Tadzhikistan

As a Raman reference standard we used a colourless hambergite crystal (2 x 2 x 1.5 cm) from the Rangkul pegmatite field, eastern Pamirs, Tadzhikistan. According to microprobe analyses, performed by Dr. Dieter Rhede (GFZ Potsdam, Germany) using the JEOL thermal field emission electron-probe JXA-8500D (HYPERPROBE) in the trace-element mode this sample contained a mean of 6.4 ± 0.3 % (g/g) F (n = 11 measurements), with a maximum of 7.1 % (g/g) (n = 2).

The sample contains fluid and melt inclusions, probably formed by phase separation. The fluid inclusions contained daughter crystals of ramanite-(Cs) and nahcolite in addition to sassolite [H_3BO_3]. According to the melting temperatures of ramanite-(Cs) and H_3BO_3, 68.1 and 61.3°C, respectively, such inclusions contain 3.4% (g/g) Cs_2O (Gmelin 1938) and 23.4 % (g/g) H_3BO_3. The melt inclusions are characterized by a vapour bubble, generally deformed, a small amount of a water-rich solution, and a large volume (~60 % (vol/vol)) of sassolite. The melting temperature of sassolite is 159 ± 15°C (n = 17), which according to Gmelin (1954) corresponds to ~72 % (g/g) H_3BO_3 or ~40 % (g/g) B_2O_3 as a first approximation, because the influence of fluorine on the melting behaviour on boric acid is unknown. Note, H_3BO_3 melts at 169 ± 1°C incongruently into HBO_2 (metaboric acid-I) and a melt with 21 ± 1 % (mol/mol) B_2O_3. At 235 ± 2°C is the eutectic point of the system HBO_2I-B_2O_3 (55.1 ± 0.5 % (mol/mol) B_2O_3. The melting point of B_2O_3 is 450 ± 2°C.

Reconnaissance homogenization measurements on 10 primary melt inclusions in hambergite from the Rangkul pegmatite give a homogenization temperature of 581 ± 15°C (see Appendix Figure 1). The homogenization is generally to the liquid state, sometimes with

critical behaviour, and in rare cases to the vapour phase. Some large inclusions decrepitated near 600°C. According to the relationship between the Mohs hardness scale and the decrepitation pressure (Tugarinov and Naumov 1970), we calculate that the pressure inside of the inclusions was about $870 \cdot 10^5$ Pa.

Just prior to total homogenisation the refraction index of the vapour bubble and the B_2O_3-rich melt are nearby identically. We observed that near homogenization the bubble or bubbles simultaneously move very rapidly inside the inclusion, implying that the viscosity of the H_2O-B_2O_3-melt must be similar to water at room-temperature: $\sim 1.00 \cdot 10^{-3}$ Pa.s.

Hambergite from the Anjanabonoina pegmatite, Madagascar

We also used a piece of a large hambergite crystal (24.3 g) from the Anjanabonoina pegmatite, Madagascar as a well characterized reference for Raman measurements (# 102984 from the Harvard Mineralogical Museum; see Dyar et al. 2001). According to microprobe measurements (see above) this sample contains 0.78 ± 0.04 % (g/g) fluorine.

In Appendix Figure 9 are shown the preliminary results of the correlation of the main Raman band of hambergite at about 153 cm^{-1} with the fluorine content (488 nm, 300 mW - about 14 mW on sample).

Appendix Figure 7

The plate shows photomicrographs of a primary melt inclusion in a growth zone of a hambergite crystal from the Rangkul pegmatite field, eastern Pamirs, Tadzhikistan taken during an homogenization experiment. At room temperature (a) the inclusion contains sassolite, a small amount of aqueous solution and a deformed vapor bubble, marked by small sassolite crystals. During heating (b, c, d) the volume of the sassolite crystals decrease slowly. At 110°C the sassolite-rich solution (L) becomes visible. The last sassolite crystal disappears at 164°C, corresponding to about 79.6 % (g/g) H_3BO_3 in the system. In the inclusion system there are only two phases: a liquid and a vapor bubble. On further heating (e, f, g) the bubble decreases steadily. At 585°C and further heating the refraction contrast between liquid and vapor gets smaller and smaller and at 587.8°C the bubble is almost invisible. At this temperature we observe boiling of the system, characterized by a rapid movement of multiple newly-formed bubbles, and their immediate disappearance (h). At 588°C is the inclusion homogenized. The process is reproducible.

Appendix Figure 8

Typical Raman spectra of hambergite, cristobalite, arsenolamprite, boric acid, and bromellite in the studied samples:

a) Raman spectra of hambergite in melt inclusions in morganite from Muiane. The bands labelled with 402Brl and 689Brl are bands of the beryl host, and Ne is a neon band.

b) Characteristic bands of cristobalite (Fig. 2b).

c) Strong diagnostic Raman bands of arsenolamprite (Fig. 2b)

d) The strong Raman bands of boric acid crystals [H_3BO_3] at 500 and 880 cm^{-1} in volatile-rich melt inclusions.

e) Diagnostic Raman bands of bromellite [BeO] at 678, 684, and 722 cm^{-1}. The intensity of these bands is so strong that the main band of beryl at 685 cm^{-1} is concealed.

Appendix Figure 9

Fluorine concentration in hambergite versus the Raman band position of the main band near 153 cm^{-1}. In the included table are given the corresponding data

Remark to diomignite [$Li_2B_4O_7 \cdot 5\ H_2O$]

London, Zolensky, and Roedder (1987) found this new mineral in crystal-rich inclusions in a spodumene sample from the Tanco pegmatite, Manitoba, Canada. However, Anderson et al. (2001) implied that diomignite had been misidentified, and that it was actually zabuyelite [Li_2CO_3]. During our Raman work on the Muiane sample we found a highly soluble mineral phase with a very strong Raman band at 1028 cm^{-1} beside weak features at 390, 446, 544, 1097 and 1352 cm^{-1}. These Raman bands, the high solubility during the spectroscopic measurements and the high boric acid concentration in the inclusion can be regarded as a second confirmation of the mineral diomignite. The identification is not simple because of the high solubility and the always coexistence with Li meta- and Li pentaborate (Gmelin 1926).

Acknowledgments

We thank Wolfgang Schmidt (Oberschöna) for the sample material from the Muiane Ta-Nb-Li-pegmatite in the Alto Ligonha region in Mozambique, as well as Dieter Rhede (GFZ Potsdam) for the hambergite sample from the Anjanabonoina pegmatite, Madagascar (#

102984) and the fluorine determination on this sample and on the hambergite sample from the Rangkul pegmatite field, eastern Pamirs, Tadzhikistan.

We thank Jake Lowenstern, George Morgan, Bryan Chakoumakos for valuable comments on an earlier version of the manuscript. Critical reviews by two anonymous reviewers, which significantly improved the quality of the manuscript, are greatly appreciated. Editorial handling by B. de Vivo and Editor-in-Chief Johann Raith are greatly acknowledged.

References

Anderson AJ, Clark AH, Gray S (2001) The occurrence and origin of zabuyelite (Li_2CO_3) in spodumene-hosted fluid inclusions: Implications for the internal evolution of rare-element granitic pegmatites. Can Miner 39: 1513-1527

Baker DR (2008) The fidelity of melt inclusions as records of melt composition: Contrib Mineral Petrol 156: 377-395

Bates JB, Quist AS (1975) Vibrational spectra of solid and molten phases of the alkali metal tetrafluoroborates. Spectrochim Acta 31A: 1317-1327

Černý P (1982) Anatomy and classifications of granitic pegmatites. MAC Short Course Handbook 8: 1-39

Černý P (2002) Mineralogy of beryllium in granite pegmatites. Rev Min 50: 405-444

Craig NC, Levin IW (1979) Calibrating Raman spectrometers with plasma lines from the argon ion laser. Appl Spectrosc 33: 475-476

Downs RT (2006) The RRUFF^{TM} Project: an integrated study of the chemistry, crystallography, Raman and infrared spectroscopy of minerals. Program and Abstracts of the 19th General Meeting of the International Mineralogical Association in Kobe, Japan. O03-13

Dyar MD, Wiedenbeck M, Robertson D, Cross L, Delaney JS, Ferguson K, Francis CA, Grew ES, Guidotti CV, Hervig RL, Hughes JM, Husler J, Leeman W, McGuire AV, Rhede D,

Rothe H, Paul RL, Richards I, Yates M (2001) Reference minerals for microanalysis of light elements. Geostand Newlett 25: 441-463

Felix M, Kiessling R (1990) Characteristics of the pegmatite-bearing area East of Marropino (Zambézia Province, P.R. of Mozambique. Z Geol Wissensch Berlin 18: 431-441

Fung DK, Voland B, Schmidt W (1990) Petrochemistry of granitoids from the Mozambique belt. Z Geol Wissensch Berlin 18: 419-429

Gmelin L (1926) Gmelins Handbuch der anorganischen Chemie, System No. 20 Lithium, Verlag Chemie, Berlin, 254 p.

Gmelin L (1930) Gmelins Handbuch der anorganischen Chemie, System No. 26 Beryllium, Verlag Chemie, Berlin, 180 p.

Gmelin L (1938) Gmelins Handbuch der anorganischen Chemie, System No. 25 Caesium, Verlag Chemie, Berlin, 268 p.

Gmelin L (1954) Gmelins Handbuch der anorganischen Chemie, System No. 13 Bor, Ergänzungsband, Verlag Chemie, Weinheim, 253 p.

Gomes CLC, Dias PA, Guimarães F, Castro P (2009) Microlites and associated oxide mineral from Naipa pegmatites – Alto Ligonha – Zambezia – Mozambique. Estudos Geológicos 19: 167-171

Grew ES (2002) Mineralogy, petrology and geochemistry of beryllium: An introduction and list of beryllium minerals. Rev Mineral 50: 1-76

Lächelt S (1990) The geologic-tectonic evolution of Mozambique as part of East Africa with special emphasis on the east Africa Rift. Z Geol Wissensch Berlin 18: 395-404

London D, Zolensky ME, Roedder E (1987) Diomignite: natural $Li_2B_4O_7$ from the Tanco pegmatite, Bernic Lake, Manitoba. Can Mineral 25: 173-180

Marshall DD, Groat LA, Falck H, Giulliani G, Neufeld H (2004) The Lened emerald prospect, Northwest Territories, Canada: Insights from fluid inclusions and stable isotopes, with implications for northern Cordilleran emerald. Can Mineral 42: 1523-1539

McMillen CD, Kolis JW (2008) Hydrothermal crystal growth of $ABe_2BO_3F_2$ (A =K, Rb, Cs, Tl) NLO crystals. Crystal Growth 310: 2033-2038

Newkirk HW, Smith DK (1965) Studies on the formation of crystalline synthetic bromellite. I. Microcrystals. Am Mineral 50: 22 - 43

Peretyazhko IS, Zagorsky, VYe (1999) Mineralogy of pegmatites. In: Shmakin BM, Makagon VM (Eds) Granitic pegmatites. Vol. 3. Novosibirsk, p. 224-389 (in Russian)

Piriou B, Videau JJ, Portier J (1981) Raman spectroscopic studies of aluminium fluoroberyllate glasses. J Non-Crystall Solids 46: 105-110

Prokofyev VJ, Peretyazhko I, Smirnov S, Tagirov BR, Groznova EO, Samsonova EA (2003) Boron and boric acid in endogenous ore-forming fluids. Moscow, 189 p. (in Russ.)

Schmidt W (1986) Geologische Entwicklung und Lagerstättenbildung der Pegmatitregion von Alto Ligonha, VR Moçambique. Dissertation B, Mining Academy Freiberg

Schmidt W, Thomas R (1990a) Zur Genesis von Seltenmetall-Granitpegmatiten auf der Grundlage von Einschlußuntersuchungen und geochemischen Betrachtungen. Z Geol Wissensch Berlin 18: 301-314

Schmidt W, Thomas R (1990b) Scheme of the genesis of Nb-Ta-pegmatites outlined by the study of inclusions. Z Geol Wissensch Berlin 18: 443-446

Schmidt C, Thomas R, Heinrich W (2005) Boron speciation in aqueous fluids at 22 to 600°C and 0.1 MPa to 2 GPa. Geochim Cosmochim Acta 69: 275-281

Switzer G, Clarke RS, Sinkankas J, Worthing HW (1965) Fluorine in hambergite. Am Mineral 50: 85 - 95

Tang D, Xia Y, Wu B, Chen C (2001) Growth of a new UV nonlinear optical crystal: $KBe_2(BO_3)F_2$. J Crystal Growth 222: 125-129

Thomas R (2000) Determination of water contents of granite melt inclusions by confocal laser Raman microprobe spectroscopy. Am Mineral 85: 868 - 872

Thomas R (2002) Determination of the H_3BO_3 concentration in fluid and melt inclusions in granite pegmatites by laser Raman microprobe spectroscopy. Am Mineral 87: 56-68

Thomas R, Davidson P (2006) Progress in the determination of water in glasses and melt inclusions with Raman spectroscopy: A short review. Z Geol Wissensch Berlin 34: 159-163

Thomas R, Davidson P (2008) Water and melt/melt immiscibility, the essential components in the formation of pegmatites; evidence from melt inclusions. Z Geol Wissensch Berlin 36: 347-364

Thomas R, Davidson P, Badanina E (2009) A melt and fluid inclusion assemblage in beryl from pegmatite in the Orlovka amazonite granite, East Transbaikalia, Russia: implications for pegmatite-forming melt systems. Min Petrol 96: 129-140

Thomas R, Davidson P, Hahn A (2008a) Ramanite-(Cs) and ramanite-(Rb): New cesium and rubidium pentaborate tetrahydrate minerals identified with Raman spectroscopy. Am Mineral 93: 1034-1042

Thomas R, Davidson P, Rhede D, Leh M (2008b) The miarolitic pegmatites from the Königshain: a contribution to understanding the genesis of pegmatites. Contrib Mineral Petrol 157: 505-523

Thomas R, Förster H-J, Heinrich W (2003) The behaviour of boron in a peraluminous granite-pegmatite system and associated hydrothermal solutions: a melt and fluid inclusion study. Contrib Mineral Petrol 144: 457-472

Thomas R, Kamenetsky VS, Davidson P (2006) Laser Raman spectroscopic measurements of water in unexposed glass inclusions. Am Mineral 91: 467-470

Thomas R, Webster JD, Davidson (2010) Be-daughter minerals in fluid and melt inclusions: implications for the enrichment of Be in granite-pegmatite systems. Contrib Mineral Petrol DOI 10.1007/s00410-010-0544-9

Thomas R, Webster JD, Heinrich W (2000) Melt inclusions in pegmatite quartz: complete miscibility between silicate melts and hydrous fluids at low pressure. Contrib Mineral Petrol 139: 394 – 401

Tugarinov AI, Naumov VB (1970) Dependence of the temperature of decrepitation on the composition of gas-liquid inclusions and on the strength of the mineral. Dokl AN SSSR, 195: 182-184 (in Russian)

Ye N, Tang D (2006) Hydrothermal growth of $KBe_2(BO_3)F_2$ crystals. J Cryst Growth 293: 233-235

Zagorsky VY, Shmakin BM (1999) Mineral composition and internal structure of pegmatites. In: Shmakin BM, Makagon VM (Eds) Granitic pegmatites. Vol. 3, Novosibirsk, p. 136-223 (in Russian.)

Figure captions

Figure 1

a) A large (405 x 240 x 350 μm) melt inclusion in a morganite crystal from the Muiane Ta-Nb-Li-pegmatite in Alto Ligonha region, Mozambique. All such melt inclusions contain a large hambergite daughter crystal [$Be_2BO_3(OH)$] and smaller daughter crystals of quartz (Qtz), cristobalite (Crs), beryl (Brl) - up to 5 % (vol/vol), a solution (L) saturated in boric acid and a large vapor bubble (V).

b) A secondary fluid inclusion (100 x 20 x 15 μm) on a healed fissure cross-cutting the growth zones, containing a saturated boric acid solution (L) (~5.5 % (g/g) H_3BO_3) with small hambergite daughter crystals (~ 1% (vol/vol)), cristobalite (Crs) and arsenolamprite (As), vapor (V), .

Figure 2

a) Typical fluid inclusion in a hambergite crystal from the Rangkul pegmatite field, eastern Pamirs, Tadzhikistan with sassolite [H_3BO_3], ramanite-(Cs) [$CsB_5O_8 \cdot 4H_2O$] and nahcolite [$NaHCO_3$]. L – solution, V –vapor.

b) Typical boric acid-rich melt inclusion in hambergite in the same crystal.

Figure 3

A volatile-rich melt inclusion in morganite, similar to Fig. 1a **(a)** after re-homogenization at 650°C and 2 kbar, this inclusion now contains silicate glass, liquid and a vapor bubble in the center. The initial hambergite crystal has dissociated and has been replaced by newly formed bromellite crystals, shown in b. The other daughter mineral phases (quartz, cristobalite, mica, topaz) and the components of the solution – boric acid and alkali borates, together with water have melted to form a silicate glass. During cooling and changes in speciation (carbonate → CO_2 and $OH^- \rightarrow H_2O$) the initially homogeneous melt was separated into a water-bearing

glass, a water-rich solution, liquid CO_2 and a CO_2-rich bubble. G- water-bearing glass, L – water-rich solution, CO_2-L – liquid CO_2, V – CO_2-rich bubble. (**b)** Close-up showing bromellite crystals in the liquid portion of the melt inclusion after cooling.

Figure 4

A volatile-rich melt inclusion in morganite with bromellite [BeO] crystals, formed from hambergite during re-homogenization at 650°C, 2 kbar in 20 hours.

G- water-bearing glass, L – water-rich solution, V – CO_2-rich bubble.

Figure 5

a) Halo of fluid and melt inclusions around two volatile-rich melt inclusions in morganite, formed by partial decrepitation during heating to 675°C and 2 kbar. Almost all of the inner inclusions contain a bromellite crystal [BeO] as shown in detail in **b)**. Immediately after the experiment the fluid inclusions in the outer ring (e.g. on the right side in **a)** contained only a solution and a bubble. However, after a period of some weeks some fluid inclusions were found to contain spontaneously crystallized bromellite crystals, suggesting metastable behaviour.

b) – f) New formed bromellite-bearing inclusions in the halo such as shown in figure **a)**. Note the large volume proportion of bromellite in the inclusions, demonstrating that the bromellite was not formed in situ from the beryl host.

BeO – bromellite, G – water-bearing glass, L – water-rich solution, V – CO_2-rich vapor.

Figure 6

A secondary fluid inclusion in morganite after heating to 650°C at 2 kbar for 20 hours with a large volume of bromellite. BeO – bromellite, L- water-rich solution

Figure 1

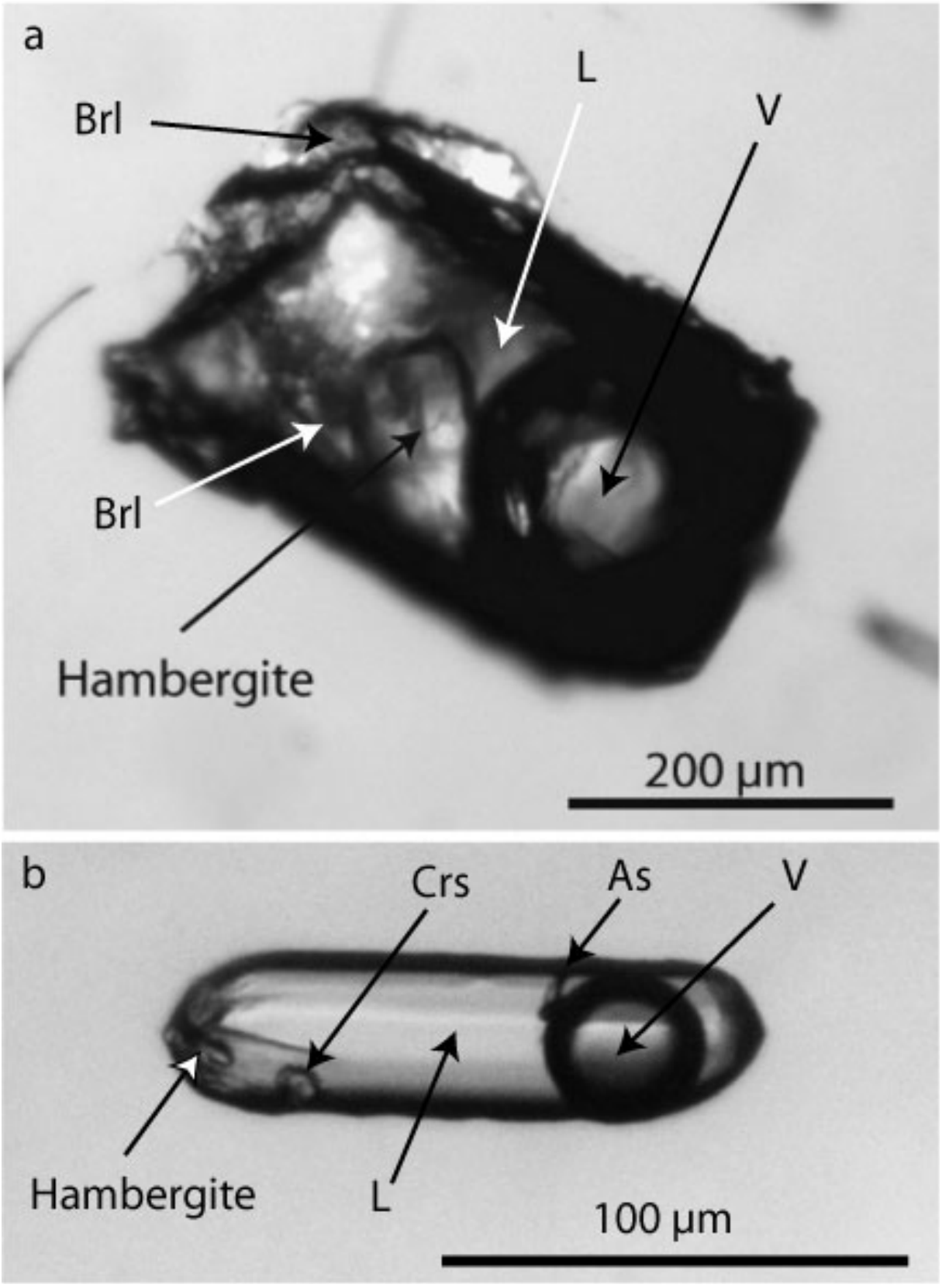

Figure 2

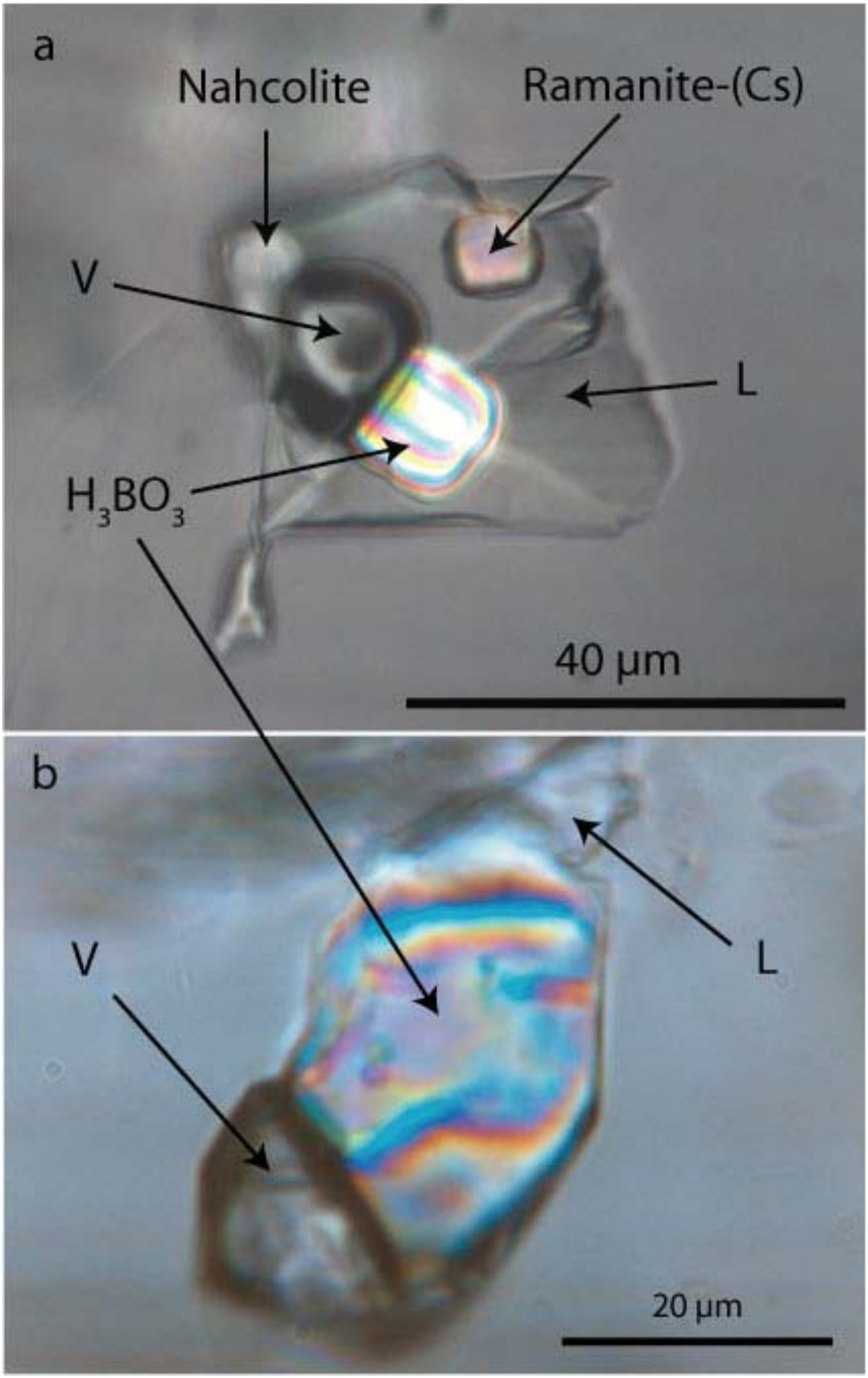

Figure 3

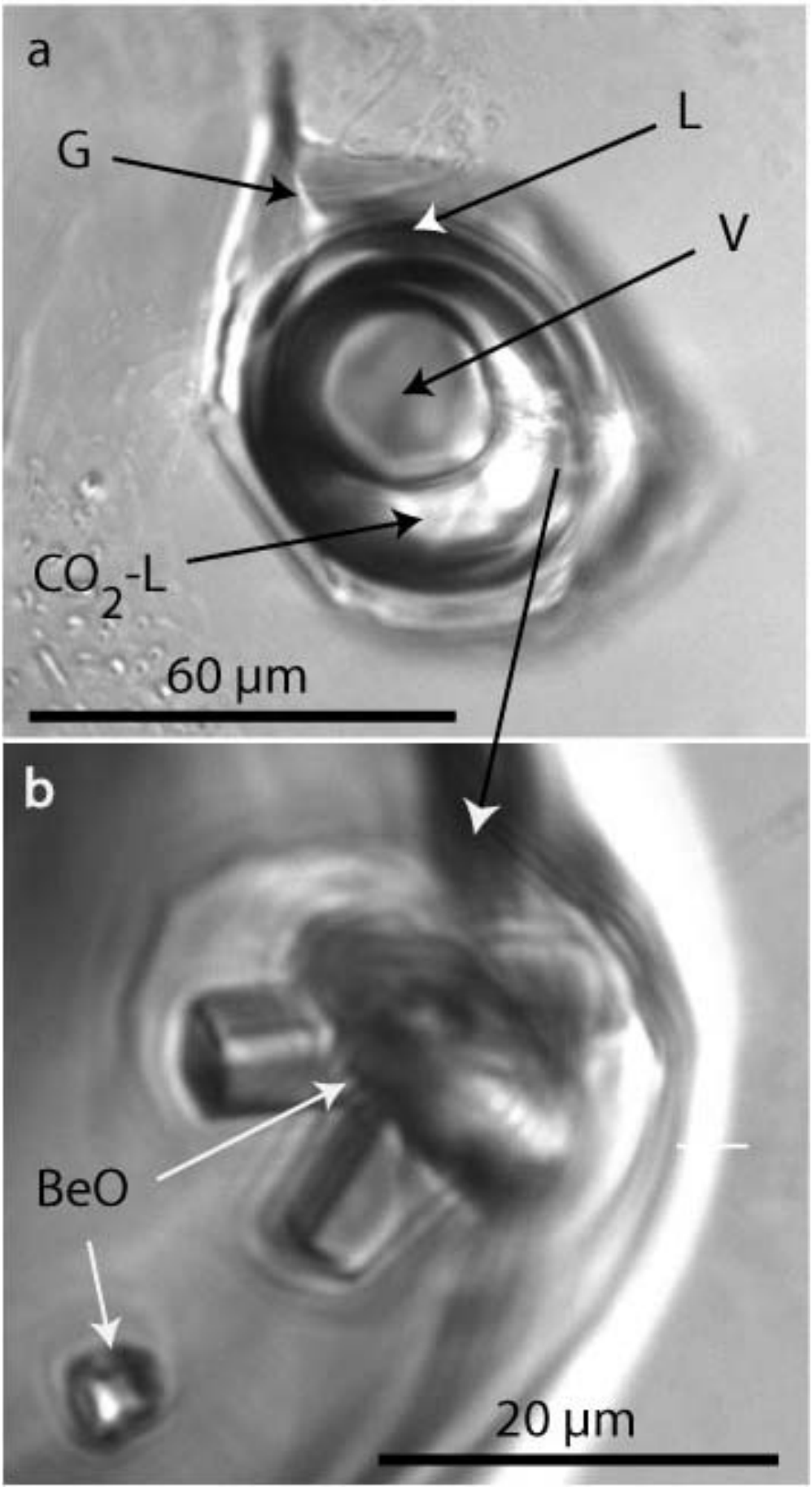

Figure 4

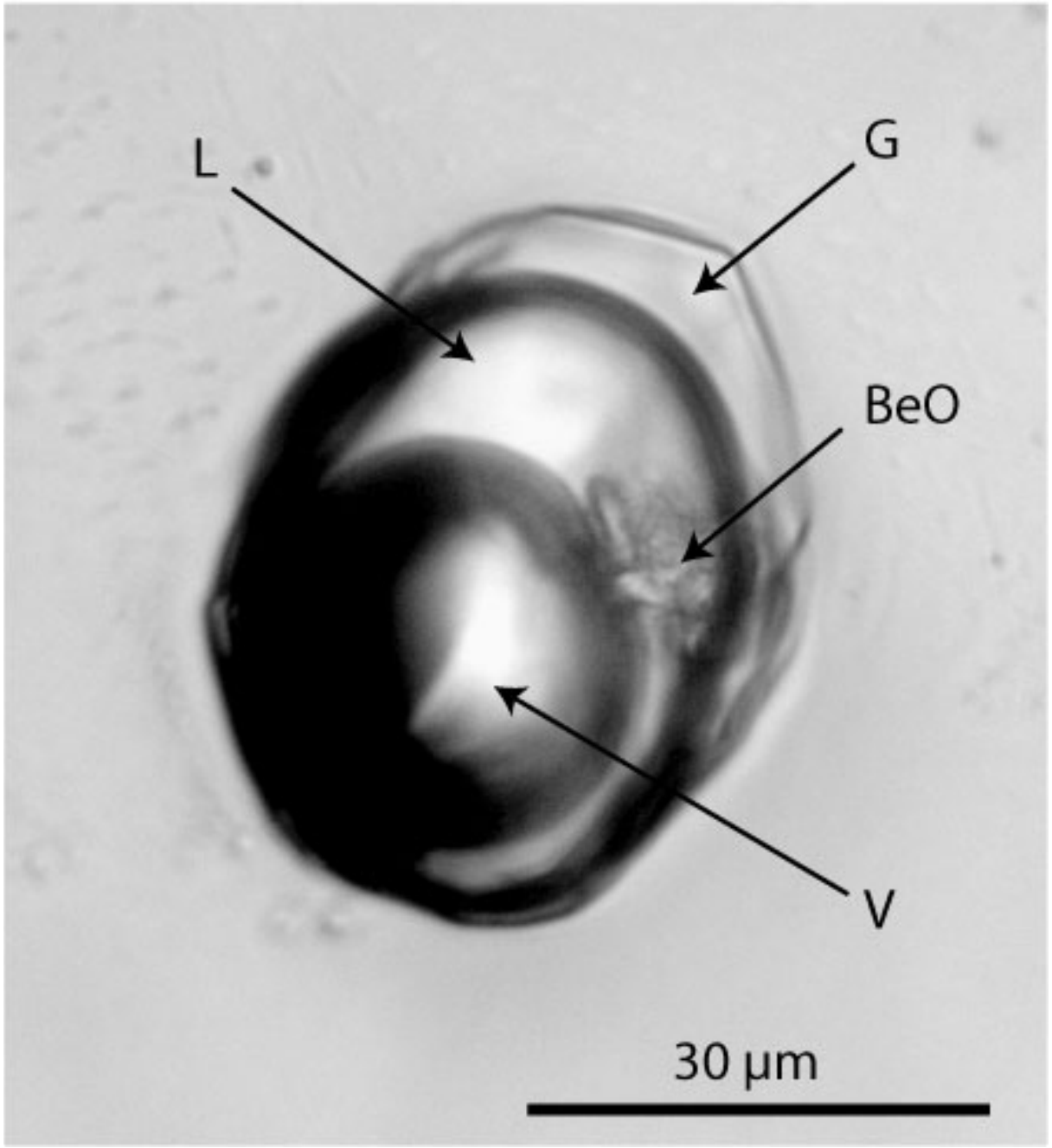

Figure 5

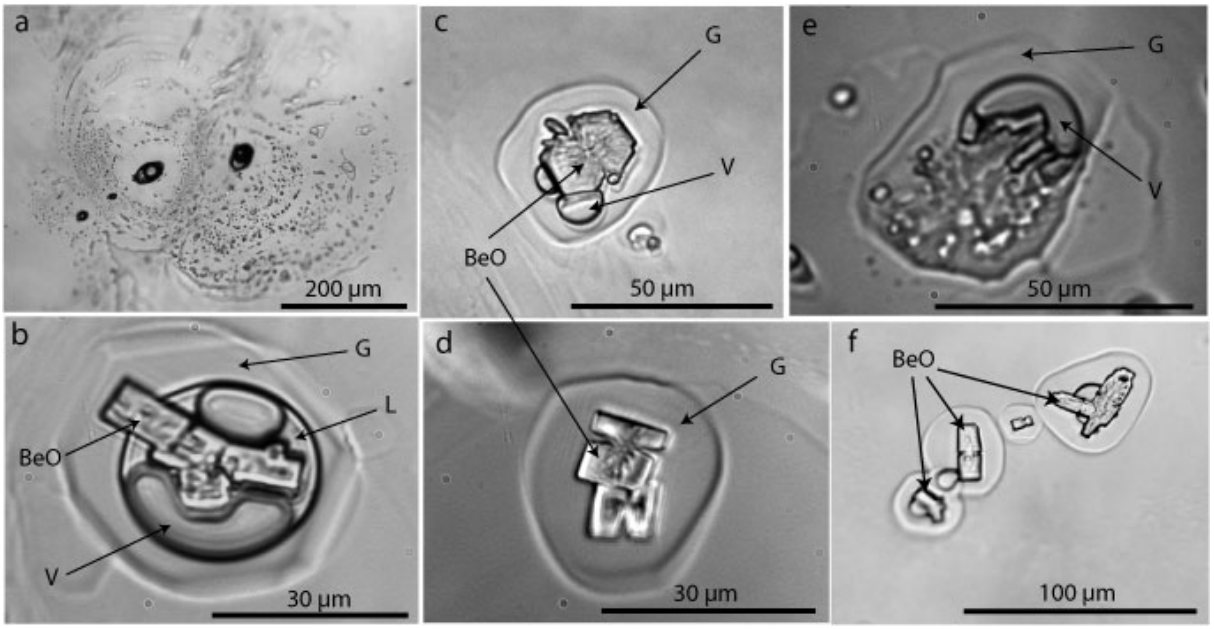

Figure 6

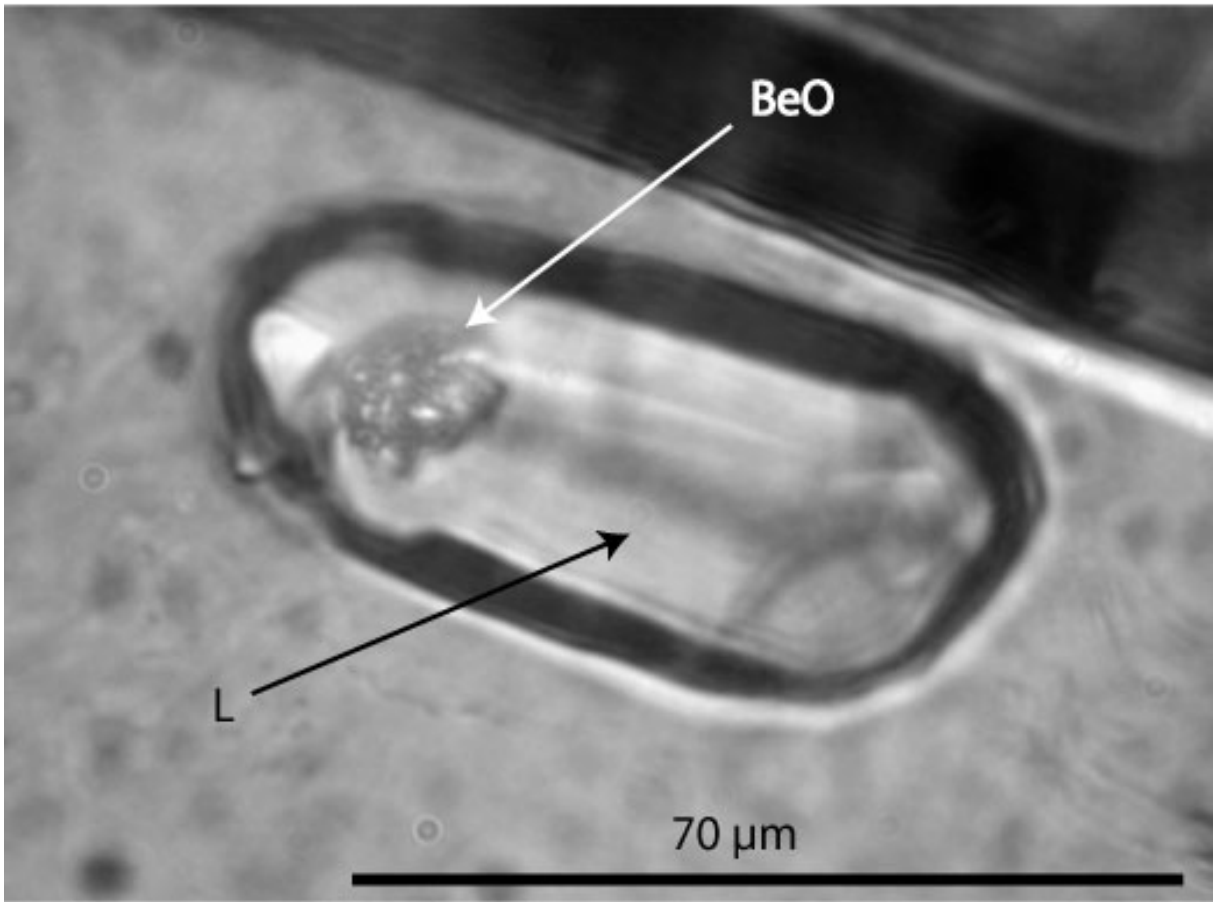

Figure 7

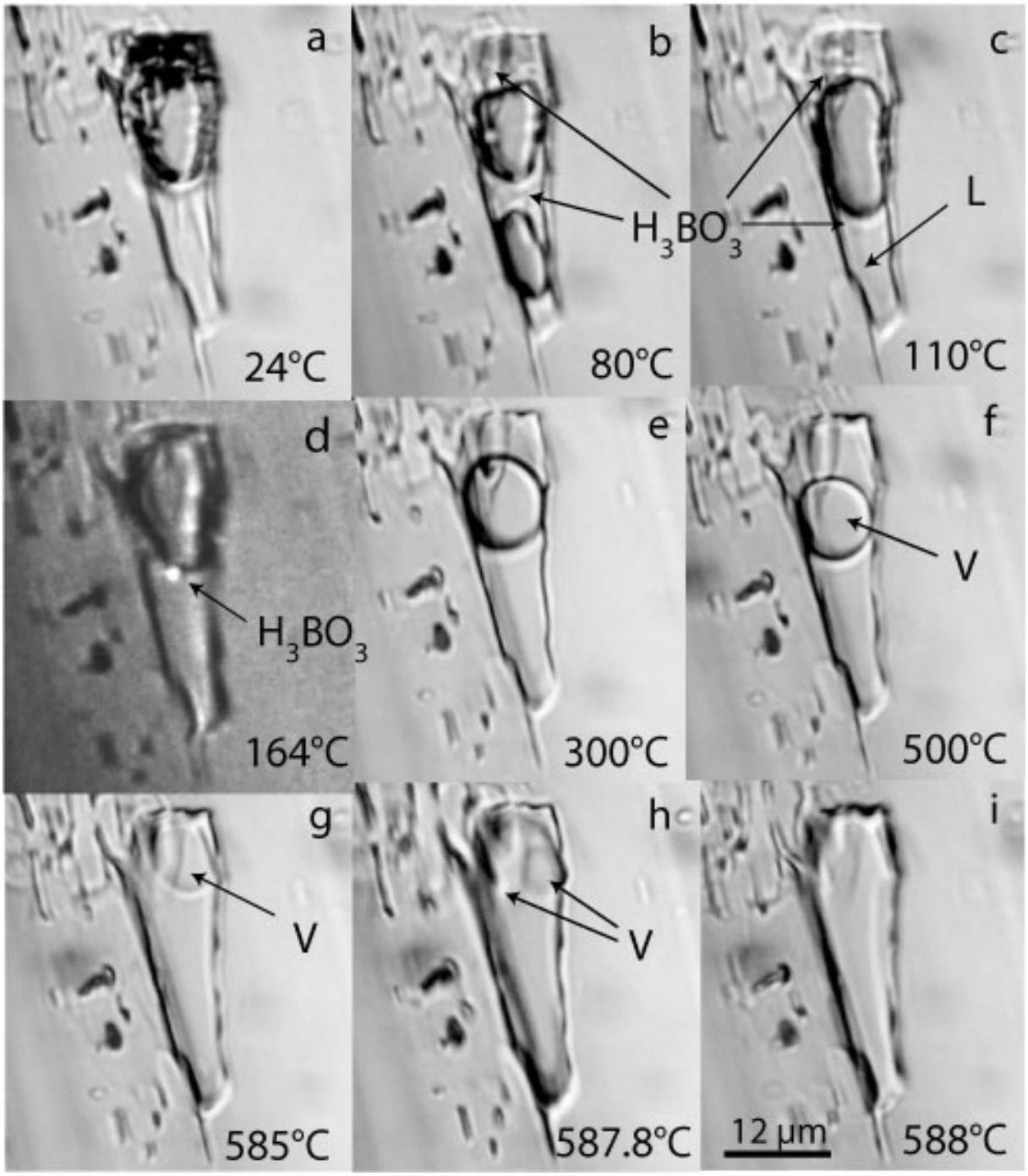
a
24°C
b
H3BO3
80°C
c
L
110°C
d
H3BO3
164°C
e
300°C
f
V
500°C
g
V
585°C
h
V
587.8°C
i
12 µm
588°C

Figure 8a-c

a)

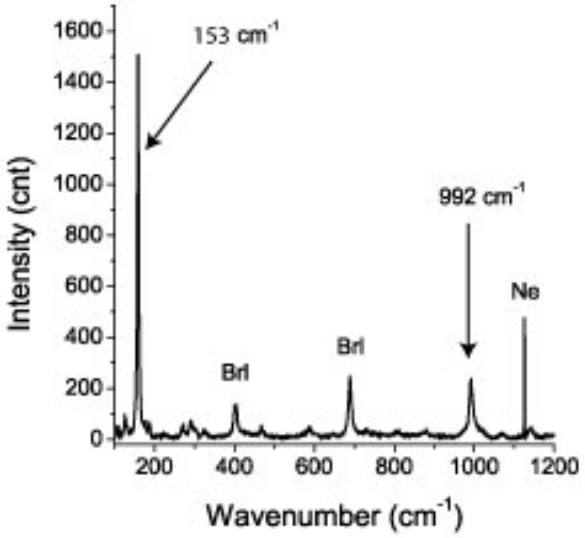

b)

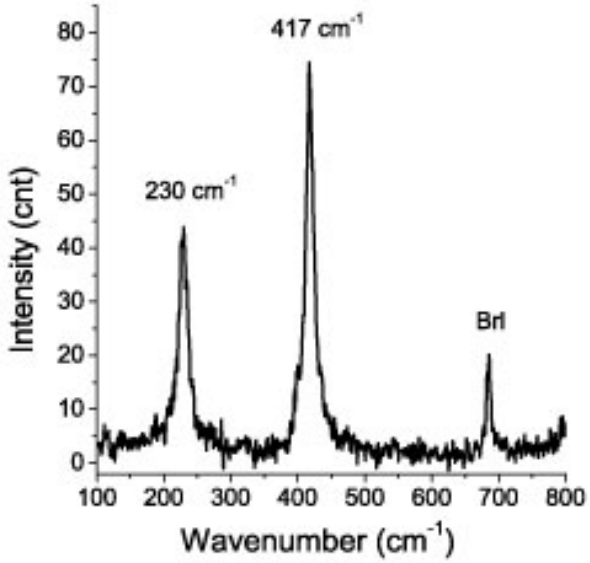

c)

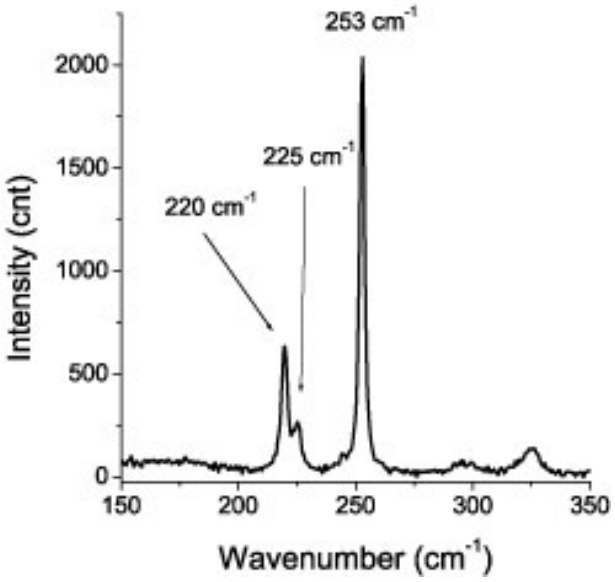

Figure 8d-e

d)

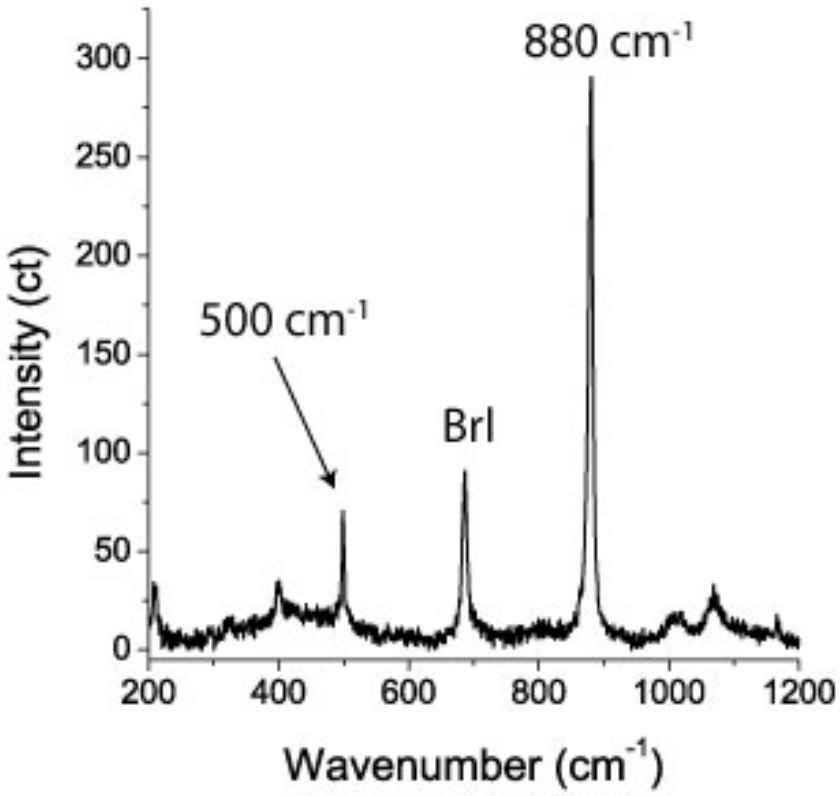

e)

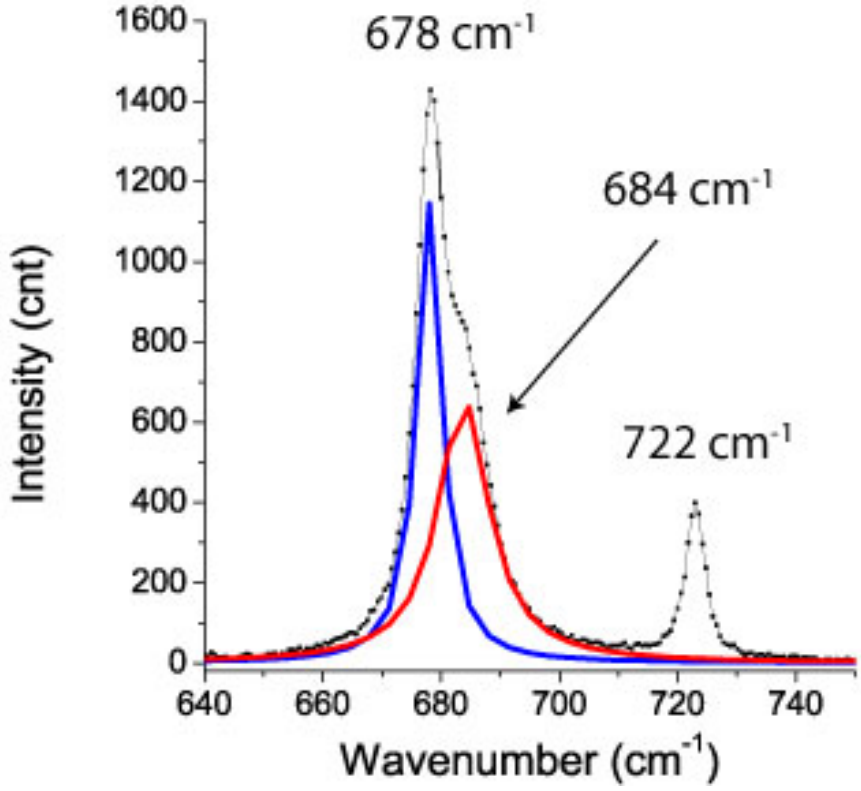

Figure 9

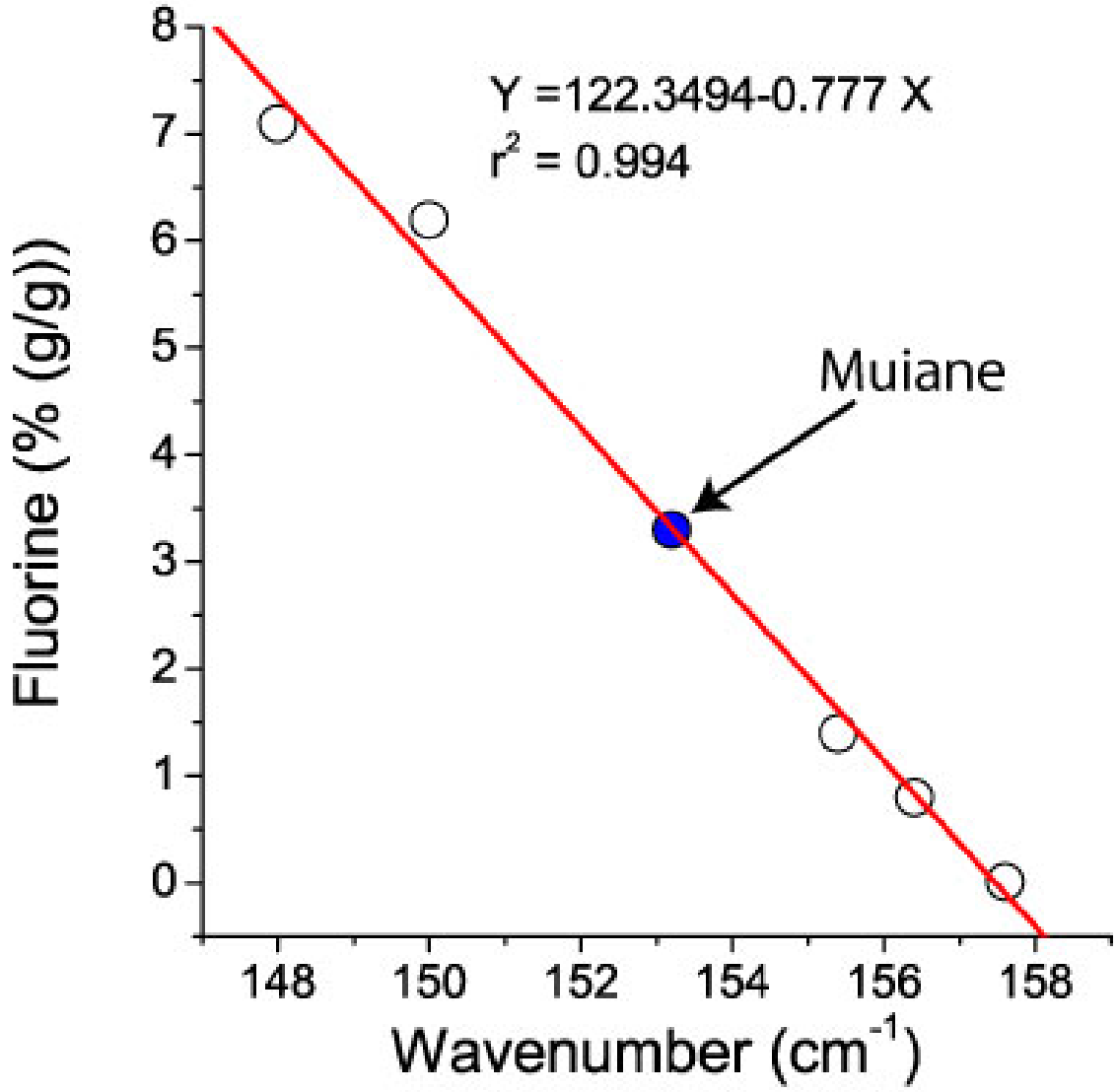

Origin	Wavenumber (cm^{-1})	F (% (g/g))
Rangkul-1	148.0	7.1
Rangkul-2	150.0	6.2
Malkhan-1	156.4	1.4
Anjanabonoina	155.4	0.8
Malkhan-2	157.6	0.01
Muiane	153.2	3.3